antibodies

Communication

Both Tumor Necrosis Factor Receptor Signaling Pathways Contribute to Mortality but not to Splenomegaly in Generalized Lymphoproliferative Disorder

Florian Wiede [1,†], Alicia Roomberg [1], Jocelyn Darby [2], Rene Gollan [1,‡] and Heinrich Körner [2,*]

[1] Comparative Genomics Centre, James Cook University, Townsville, Qld 4811, Australia;
E-Mails: florian.wiede@monash.edu (F.W.); aliciaroomberg@live.com (A.R.);
Rene.Gollan@unimedizin-mainz.de (R.G.)

[2] Heinrich Körner, Menzies Research Institute Tasmania, Medical Science 2, 17 Liverpool Street, Hobart, Tasmania 7000, Australia

[†] Current address: Cellular Signaling and Human Disease Laboratory, Department of Biochemistry & Molecular Biology, Monash University, VIC 3800, Australia.

[‡] Current address: Klinik und Poliklinik für Neurologie, Johannes Gutenberg-Universität, D-55131 Mainz, Germany.

[*] Author to whom correspondence should be addressed; E-Mail: heinrich.korner@utas.edu.au; Tel.: +61-3-62264698; Fax: +61-3-62267704.

Academic Editor: Dimiter S. Dimitrov

Abstract: The phenotypical consequences of a combined deficiency of the Fas-Fas Ligand (FasL) and one or both Tumor Necrosis Factor (TNF) signaling pathways were investigated. Mice, which expressed a non-functional FasL suffered from a pathological accumulation of both B and T cells leading to splenomegaly and lymphadenopathy and, depending on the genetic background, pathogenic self-reactive antibodies (*generalized lymphoproliferative disorder (gld)*-phenotype). If mice additionally lacked TNF, they displayed a significantly ameliorated *gld*-phenotype while TNF Receptor-1-deficient *gld* mice (B6.*gld*.TNFR1$^{-/-}$) displayed a more severe phenotype. To complement this combination, we also generated TNF Receptor-2-deficient *gld* mice (B6.*gld*.TNFR2$^{-/-}$). Both double knockouts followed in their splenic structure the respective TNFR contribution to the phenotype. TNFR1$^{-/-}$ mice showed an absence of B cell follicles in the spleen while TNFR2$^{-/-}$ mice were comparable

to WT mice. In general, we demonstrated a strong contribution of both TNFR signaling pathways to the symptoms of *gld* with the notable exception of splenomegaly where only TNFR1$^{-/-}$ played a role.

Keywords: autoimmunity; tumor necrosis factor; tumor necrosis factor receptor; gene-deficient models

1. Introduction

Apoptosis is fundamental for the maintenance of both central and peripheral tolerance and the contraction of effector responses in the periphery [1]. Consequently, inhibition of apoptosis leads to lymphoaccumulation and a predisposition to autoimmune disease [2]. Apoptosis facilitates cellular homeostasis in the immune system via the extrinsic pathway [1,3], which is triggered by cytokines of the TNF family of ligands [4,5]. More specifically, the pro-apoptotic cytokine FasL is expressed on a variety of immune cells such as CD8$^+$ T cells and is involved in the induction of apoptosis via its cognate receptor Fas (FasR) [1]. Two different spontaneous recessive murine mutations have been described that caused the adjournment of immune homeostasis and resulted in massive lymphoaccumulation accompanied by symptoms of an autoimmune disorder comparable to Systemic Lupus Erythematosus (SLE) [6,7]. Consequently, these mutation-carrying strains have been named *lymphoproliferation* (*lpr*) and *generalized lymphoproliferative disorder* (*gld*) [7]. As underlying cause of the disorders a complete loss of Fas as well as a loss-of-function mutation of FasL have been identified [5]. Another member of the TNF family, the name giving cytokine TNF, can also trigger apoptosis via the TNFR1 [8]. The involvement of TNFR-1 in the *lpr* phenotype has been analyzed and an additive pathological activity of Fas and TNFR1 has been demonstrated [9] while a combination of *gld* and TNF resulted in an attenuated form of lymphadenopathy [10]. To further dissect the signaling pathways involved in the autoimmune pathogenesis of the *gld* mouse strain *gld*.TNFR1$^{-/-}$ and *gld*.TNFR2$^{-/-}$ knockout mouse strains were generated and their phenotype was analyzed to compare the phenotypic outcomes from the loss of these receptors.

2. Results and Discussion

2.1. Comparison of the Overall Phenotype of B6.gld.TNFR1$^{-/-}$ and B6.gld.TNFR2$^{-/-}$ Mice

We analyzed the phenotypical consequences of the deletions of *tnfr1* and *tnfr2* in combination with the loss-of-function of *fasL* and tested the B6.*gld*.TNFR1$^{-/-}$ and B6.*gld*.TNFR2$^{-/-}$ mouse strains [9,10] for the influence of these combined mutations on hallmarks of the *gld* phenotype: The long term survival of the mice and the extent of the splenomegaly. Furthermore, we determined the splenic CCL21 expression because specifically the absence of TNF prevents the expression of this chemokine in B6.*gld*.TNF$^{-/-}$ mice [11].

Interestingly, the length of survival of the two genotypes was very similar (Figure 1A) and a comparison to previously published data showed that it was not significantly different from the B6.*gld* strain but shorter than B6.*gld*.TNF$^{-/-}$ mice ((B6.*gld*.TNFR1 and 2$^{-/-}$ strain: 40 weeks 50% survival; B6.*gld*.TNF$^{-/-}$ mice: 70 weeks 50% survival; [12]). We could not detect a significant difference between the survival times of male and female B6.*gld*.TNFR1$^{-/-}$ mice (males: n = 20; females: n = 8) using a log rank (Mantel-Cox) test or Gehan-Breslow Wilcoxon test.

(A)

(B)

(C)
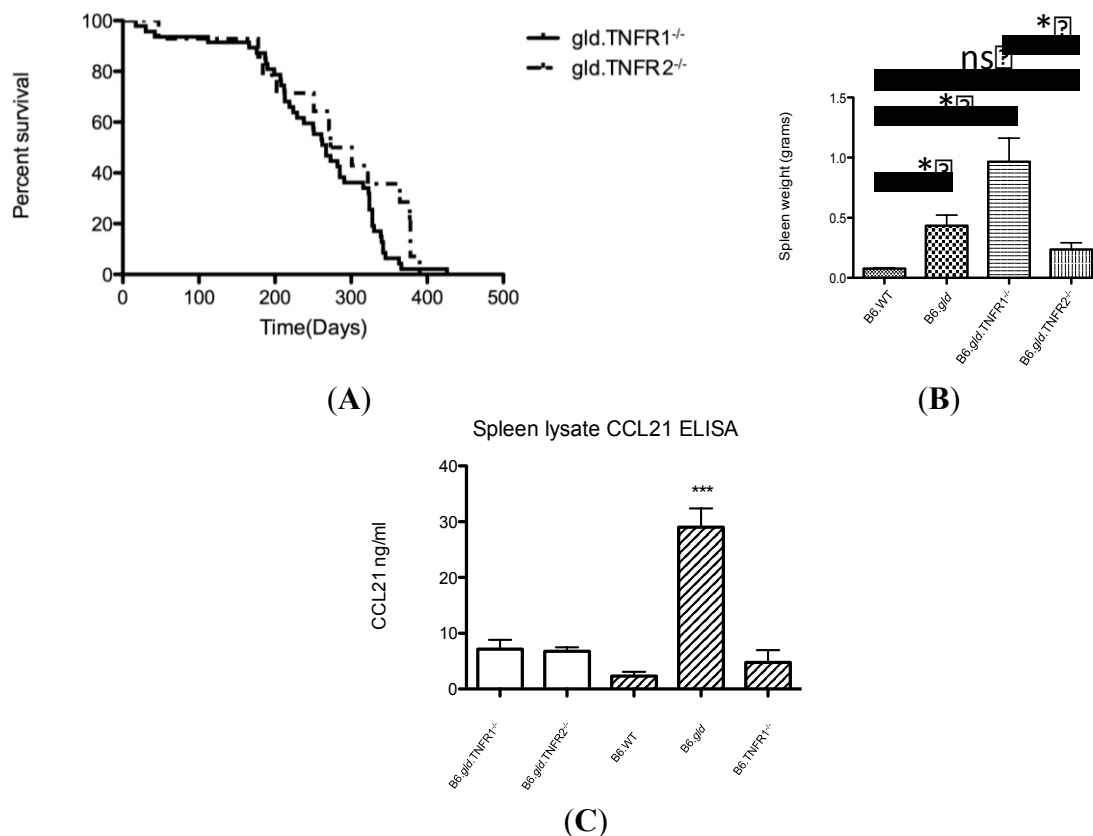
Figure 1. Comparative analysis of B6.*gld*.TNFR1$^{-/-}$ and B6.*gld*.TNFR2$^{-/-}$ mice with regard to morbidity, spleen weight, intracellular cytokine FACS and chemokine ELISA: (**A**) A similar progression of the clinical *gld* syndrome is observed in both B6.*gld*.TNFR1$^{-/-}$ and B6.*gld*.TNFR2$^{-/-}$ mice. An analysis of a survival curve with both a log rank (Mantel-Cox) test or Gehan-Breslow Wilcoxon test did not demonstrate a significant difference between the two genotypes (B6.*gld*.TNFR1$^{-/-}$ mice: n = 47; B6.*gld*.TNFR2$^{-/-}$ mice: n = 19); (**B**) The B6.*gld*.TNFR1$^{-/-}$ mice develop a significantly larger spleen. A comparison of WT (n = 3), *gld* (n = 6), B6.*gld*.TNFR1$^{-/-}$ (n = 22) and B6.*gld*.TNFR2$^{-/-}$ mice (n = 15) showed a significant larger spleen in the B6.*gld*.TNFR1$^{-/-}$ strain as compared to B6.WT or B6.*gld*.TNFR2$^{-/-}$ spleens (one way Anova, p ≤ 0.001). All spleens in this comparison were harvested for this publication. *: p ≤ 0.05; ns: not significant; (**C**) The expression of CCL21 in the spleen is intermediate in both B6.*gld*.TNFR1$^{-/-}$ and B6.*gld*.TNFR2$^{-/-}$ mice (white bars). The titre of CCL21 in spleen tissue was determined by ELISA and was found to be 9.5 (n = 19) and 7 ng/mL (n = 15), respectively. The data for B6.WT, B6.*gld* and B6.TNFR1 (striped bars) were published previously and were added to this figure as comparison [12], ***: p ≤ 0.01.

In contrast, the size of the spleens was markedly different between the B6.*gld*.TNFR1$^{-/-}$ and B6.*gld*.TNFR2$^{-/-}$ mouse strains. While the spleens of the B6.*gld*.TNFR1$^{-/-}$ mice almost reached the size of B6.*gld* spleens [9] the B6.*gld*.TNFR2$^{-/-}$ spleens remained relatively small and were found to be only marginally bigger than B6.WT spleens (Figure 1B). The substantial size difference of spleens from B6.*gld*.TNFR1$^{-/-}$ (Figure 1B) and B6.*gld* mice [12] which were bred in our animal facility to previously published data of MRL.*lpr*.TNFR1$^{-/-}$ mice [9] can be explained with the increased susceptibility of the MRL strain to the development of the autoimmune phenotype in general, and of splenomegaly and lymphadenopathy, in particular [7]. A phenotypic comparison of the TNFR1$^{-/-}$ and TNFR2$^{-/-}$ mice was not carried out. A gross analysis of the cellularity of the spleen of both genotypes has been published previously [13] and could not find a difference to the WT strain [14].

Previously it has been shown that B6.*gld* mice overexpress CCL21 and that the absence of TNF specifically prevents this overexpression reducing autoimmune pathology [11]. It was hypothesized that this TNF-dependent CCL21 expression was one of the underlying causes of the accumulation of T cells and B cells in the peripheral lymphoid organs. Since the B6.*gld*.TNFR1$^{-/-}$ and B6.*gld*.TNFR2$^{-/-}$ mouse strains displayed a significant difference in the size of their spleen we tested the expression of CCL21 in these mouse strains using a CCL21-specific capture ELISA as compared to B6.WT, B6.*gld* and B6.TNFR1$^{-/-}$ genotypes which had been published previously [11,12]. It showed that the expression level of CCL21 in B6.*gld*.TNFR1$^{-/-}$ and B6.*gld*.TNFR2$^{-/-}$ mouse spleens was not significantly different from each other or from B6.WT spleens but substantially lower as in B6.*gld* mice (Figure 1C).

The cytokine TNF and its pro-inflammatory receptor TNFR1 are central for a protective innate immune response in particular to intracellular pathogens such as parasites [15] or bacteria [16] while the functions of the second TNF signaling pathway are still not entirely resolved and are probably involved in immune homeostasis [17]. However, the pro-inflammatory signaling pathway is also associated with chronic inflammation, which is observed in autoimmune diseases such as inflammatory bowel disease (IBD) or rheumatoid arthritis or in a mouse model of systemic lupus erythematosus, *gld* [16]. The combination of different gene-deficient strains allowed us to investigate how either of the two TNFR-pathways or a combination of both contributed to the severe autoimmune disorder *gld* caused by the absence of a functional FasR-FasL signaling transduction. First, a TNFR1 deficiency on a *gld*.MRL background leads to a stronger and more accelerated phenotype with a more pronounced splenomegaly and increased titres of autoantibodies [9]. Our results confirm this outcome to some extent but put some emphasis back on the role of the MLR background, which has been described as autoimmune-prone [18,19]. In this comparative study of B6.*gld*.TNFR1$^{-/-}$ mice we observe a longer mean survival time than B6.*gld* mice and significant splenomegaly and lymph node hypertrophy contrasted with a normal CCL21 expression [10,11]. This could be explained because the absence of TNFR1 can be responsible for the increased activation of TNFR2 signaling pathways [20] and it could lead to an increased proliferation of T cells [21]. Concurrently, the higher level of NF-kB activation could also antagonize the TNF-induced TNFR2-mediated apoptosis and thus cause lymphoaccumulation [22]. Second, a previously published investigation of the *gld*/TNF$^{-/-}$ phenotype on a B6 background showed a strong attenuation of the *gld* symptoms and an absence of splenomegaly [10]. This phenotype could have been caused by the absent proliferative signal through the TNF-TNFR2 signaling pathway and the loss of the anti-apoptotic

influence of TNF on T cells [10]. Consequently, we had hypothesized that TNFR2 contributed significantly to the observed autoimmune symptoms and we concluded that a combination of a TNFR2-deficient mouse strain with *gld* would abrogate most of the phenotype and would be more benign in its phenotype. This was only the case with regard to splenomegaly but not the survival time of B6.*gld*.TNFR2$^{-/-}$ mice.

2.2. Transfer of CD4$^-$/CD8$^-$ DN T Cells into TNFR Double Knockouts Follows the Respective TNFR Phenotype and Results in Migration to the Bridging Channels or Ends in the B Cell Area

The separation and shape of T and B cell areas in the spleen are changed by TNF [23] or TNFR1 gene-deficiencies [24] and well-defined B cell follicles are replaced by rim-like B cell structures. (Figure 2C; [23,25]). In B6.*gld* and B6.*gld*.TNF$^{-/-}$ mice an additional population of T cells is detectable that is double negative (DN) for CD4 and CD8 [26]. Previous experiments have shown that the DN T cell populations of B6.*gld* and B6.*gld*.TNF$^{-/-}$ mice were positive for CXCR5 and migrated *in vitro* in response to CXCL13 but did not express CCR7 [11,27]. After adoptive transfer into a wildtype mouse this population stopped at the splenic bridging channel and proceeded only very slowly into the follicle despite the expression of CXCR5 [27]. This DN T cell population was isolated using flow cytometry, labeled with CFSE and used to test the contribution of structures such as follicles and bridging channels to the cell migration in B6.*gld*.TNFR1$^{-/-}$ and B6.*gld*.TNFR2$^{-/-}$ mouse spleens. The control transfer of DN T cells into B6.WT confirmed the stop at the bridging channels (Figure 2A). In TNF- and TNFR-deficient mice the migration patterns of DN T cells followed the structure of the follicles. The spleens of B6.*gld*.TNFR1$^{-/-}$ and B6.*gld*.TNF$^{-/-}$ mice displayed rim-like B cell structures without follicular compartmentalization and the DN T cells entered the B cell area without further delay and were distributed evenly throughout the B cell area (Figure 2C,D). In contrast, B6.*gld* and B6.*gld*.TNFR2$^{-/-}$ spleens showed a follicular structure comparable to B6.WT spleens. In these genotypes the transferred DN T cells relocated accordingly and paused at the bridging channels (Figure 2B,E).

In a previous study we had correlated the expression of CCL21 with the *gld*-phenotype and had been able to demonstrate that the additional absence of TNF, which caused the disruption of both TNFR signaling pathways and a significant reduction of the CCL21 expression, resulted in a more benign pathology [11]. The implied causal connection between chemokine expression and autoimmune pathology has to be reconsidered. In our current study we show a comparable expression of the chemokine CCL21 in both B6.*gld*.TNFR1$^{-/-}$ and B6.*gld*.TNFR2$^{-/-}$ spleen yet significantly different cellularity of the lymphoid organs, which is contrasted by migration of DN T cells that purely followed the structure of the splenic architecture. To finally address this question about an influence of CCL21 on the *gld*-pathology we will need to overexpress the chemokine in the absence of TNF.
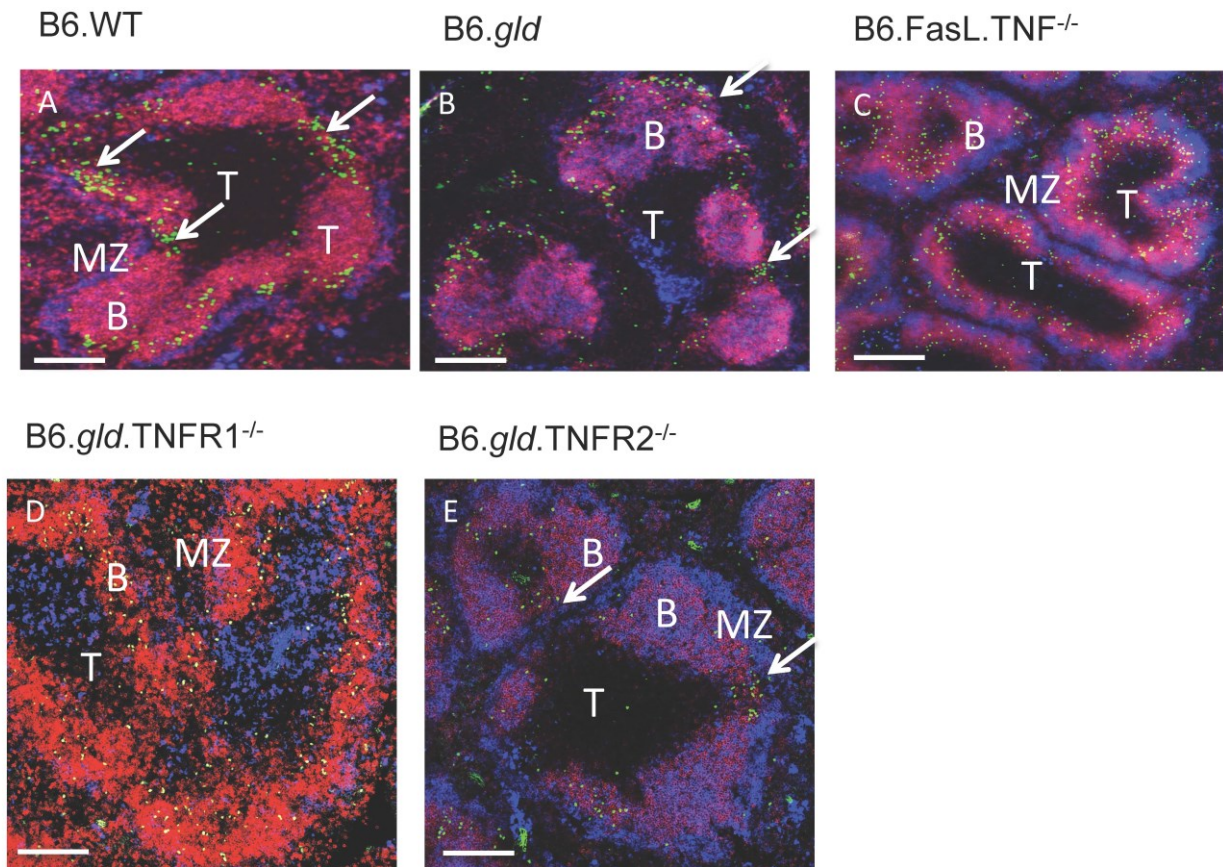
Figure 2. The spleen phenotype is determined by TNF-TNFR signaling. B6.WT (**A**), B6.*gld* (**B**), B6.*gld*.TNF$^{-/-}$ (**C**), B6.*gld*.TNFR1$^{-/-}$ (**D**) and B6.*gld*.TNFR2$^{-/-}$ (**E**) spleens were analyzed histologically after transfer of CFSE-labeled DN T cells. Using mAbs for IgM (red) and IgD (blue) the outline of the T cell area (T), B cell follicles (F) and the marginal zone (MZ) were determined. The bridging channels (arrows) are clearly visible in B6.WT, B6.*gld*, and B6.*gld*.TNFR2$^{-/-}$ spleens (10× objective magnification). The scale bar equates to 250 μm.

3. Experimental Section

3.1. Mouse Strains

The C57Bl/6(B6).*gld*.TNFR1$^{-/-}$ and B6.*gld*.TNFR2$^{-/-}$ mouse strains were established by backcrossing B6.*gld* [7] with B6.TNFR1$^{-/-}$ or B6.TNFR2$^{-/-}$ deficient mice, respectively [13] followed by inter-crossing of F1 progeny to achieve homozygosis. Mice homozygous for both the *gld* mutation and TNFR1 or TNFR2 deficiency were selected using screening primers outlined in previous publications [13,28]. Additional mouse strains used were B6.FasL.TNF$^{-/-}$ [10] and B6.TNF$^{-/-}$ [23]. The genetically unmodified mouse strain C57BL/6 was used as control. All animals were kept under specific pathogen free conditions in IVC units at the animal research facilities of the Comparative Genomics Centre, James Cook University, Townsville, Australia and the Menzies Research Institute Tasmania, Hobart, Australia. Mice used for the phenotypic comparison (Figure 1) were kept Comparative Genomics Centre, James Cook University, Townsville. Mice of both sexes were used.

3.2. Ethics Statement

Care of animals was in accord with institution guidelines of James Cook University, Townsville and the University of Tasmania, Hobart.

3.3. CCL21 Elisa

The amount of CCL21 in spleen tissue was determined as described [11] using a Capture-ELISA with purified and biotinylated CCL21 specific antibodies for capture and detection, respectively (R&D Systems, Minneapolis, MN, USA), and recombinant murine CCL21 (R&D Systems) as standard. The resulting chemokine concentration was normalized by tissue weight.

3.4. Fluorescence Immunohistology

Spleens were harvested, frozen in Optimal Cutting Temperature (OCT) medium and cut in sections (8 μm). Fluorescence immunohistology was performed as described in detail elsewhere [29]. Antibodies used were: Rat anti mouse μ heavy chain (Cy5), rat anti mouse δ heavy chain, rat anti-mouse B220 (purified or biotinylated; clone RA3-6B2; BD Biosciences). Biotinylated B220 was revealed using Streptavidin Alexa 594 or 546, respectively. Purified B220 was revealed with goat anti rat Alexa 488 (Invitrogen, Sydney, Australia). The sections were analyzed using an Olympus BX51 microscope (Olympus, Sydney, Australia) with a high-sensitivity gray-scale digital camera (Olympus Optotronics, Olympus) and Magnifier software (Olympus).

3.5. Flow Cytometry

The cells were stained for CD4 (RM4-5, PerCP-Cy5.5) and CD3 (145-2C11, APC-Cy7). Intracellular cytokine flow cytometry was performed as described in detail elsewhere [10] using Cytofix-Cytoperm (BD Biosciences, North Ryde, NSW, Australia) following the manufacturer's instructions and rat anti mouse IFN-γ (XMG1.2, Alexa Fluor-488). Data were collected using a FACS-Calibur flow cytometer and analyzed with Cell-Quest software (BD Biosciences).

3.6. Adoptive Cell Transfer

Lymphocytes were harvested from spleens and lymph nodes of B6.*gld* mice and $CD4^- CD8^- TCR^+$ T cells were isolated using a BD Aria cell sorter (BD Biosciences). The T cells were labelled with carboxyfluorescein diacetate succinimidyl ester (CFSE; Molecular Probes, Invitrogen) as described [30] and transferred intravenously into B6.WT, B6.*gld*, B6.*gld*.$TNF^{-/-}$, B6.*gld*.$TNFR1^{-/-}$ and B6.*gld*.$TNFR2^{-/-}$ mice. The spleens of the recipients were harvested 16–24 h after transfer and analysed using immunofluorescence after a co-staining with anti μ and δ heavy chain antibodies.

4. Conclusions

Our investigation of B6.*gld*.$TNFR1^{-/-}$ and B6.*gld*.$TNFR2^{-/-}$ mice has demonstrated that the clinical outcome in both genotypes followed the respective phenotype, which had been caused by either a

deficient TNF-TNFR1 or TNF-TNFR2 signaling pathway. Both genotypes expressed CCL21 at WT level, but while B6.*gld*.TNFR1$^{-/-}$ mice showed a modified spleen structure comparable to the TNF-knockout the B6.*gld*.TNFR2$^{-/-}$ strain resembled a WT spleen. The data presented formally prove that the presence of the TNF-TNFR2 axis alone contributes to an augmentation of the disorder while the sole presence of TNF-TNFR1 abolishes some effects of the consequences of an inactive FasL such as splenomegaly. Interestingly, a complete absence of TNF signaling does attenuate the *gld* phenotype which points again at an actively detrimental role of an existing TNF-TNFR2 signaling pathway but could also be due to the anti-apoptotic effect TNF has specifically on T cells. Taken together, we demonstrate that an intact TNFR1 pathway (maintained in the B6.*gld*.TNFR2$^{-/-}$ strain) plays a significant role in the prevention of splenomegaly, which is typical for the *gld* phenotype. For the first time we are able to formally proof that in the absence of the TNF-TNFR2 signaling pathway splenomegaly is prevented yet survival is still reduced.

Acknowledgments

Author Contributions

F.W. and H.K. designed the study; F.W., A.R., J.D., R.G. and H.K. produced and analysed the data; H.K. prepared the manuscript.

Conflicts of Interest

The authors declare no conflict of interest.

References

1. Strasser, A.; Jost, P.J.; Nagata, S. The Many Roles of FAS Receptor Signaling in the Immune System. *Immunity* **2009**, *30*, 180–192.
2. Rathmell, J.C.; Thompson, C.B. Pathways of apoptosis in lymphocyte development, homeostasis, and disease. *Cell* **2002**, *109*, S97–S107.
3. Cohen, P.L.; Eisenberg, R.A. The lpr and gld genes in systemic autoimmunity: Life and death in the Fas lane. *Immunol. Today* **1992**, *13*, 427–428.
4. Lynch, D.H.; Ramsdell, F.; Alderson, M.R. Fas and FasL in the homeostatic regulation of immune responses. *Immunol. Today* **1995**, *16*, 569–574.
5. Nagata, S. Fas and Fas ligand: A death factor and its receptor. *Adv. Immunol.* **1994**, *57*, 129–144.
6. Pisetsky, D.S.; Caster, S.A.; Roths, J.B.; Murphy, E.D. Ipr gene control of the anti-DNA antibody response. *J. Immunol.* **1982**, 128, 2322–2325.
7. Roths, J.B.; Murphy, E.D.; Eicher, E.M. A new mutation, gld, that produces lymphoproliferation and autoimmunity in C3H/HeJ mice. *J. Exp. Med.* **1984**, *159*, 1–20.
8. Tartaglia, L.A.; Rothe, M.; Hu, Y.F.; Goeddel, D.V. Tumor necrosis factor's cytotoxic activity is signaled by the p55 TNF receptor. *Cell* **1993**, *73*, 213–216.

9. Zhou, T.; Edwards, C.K., 3rd; Yang, P.; Wang, Z.; Bluethmann, H.; Mountz, J.D. Greatly accelerated lymphadenopathy and autoimmune disease in lpr mice lacking tumor necrosis factor receptor I. *J. Immunol.* **1996**, *156*, 2661–2665.

10. Körner, H.; Cretney, E.; Wilhelm, P.; Kelly, J.M.; Röllinghoff, M.; Sedgwick, J.D.; Smyth, M.J. Tumor necrosis factor sustains the generalized lymphoproliferative disorder (gld) phenotype. *J. Exp. Med.* **2000**, *191*, 89–96.

11. Wiede, F.; Vana, K.; Sedger, L.M.; Lechner, A.; Körner, H. TNF-dependent overexpression of CCL21 is an underlying cause of progressive lymphoaccumulation in generalized lymphoproliferative disorder. *Eur. J. Immunol.* **2007**, *37*, 351–357.

12. Wiede, F.; Roomberg, A.; Cretney, E.; Lechner, A.; Fromm, P.; Wren, L.; Smyth, M.J.; Korner, H. Age-dependent, polyclonal hyperactivation of T cells is reduced in TNF-negative gld/gld mice. *J. Leukoc. Biol.* **2009**, *85*, 108–116.

13. Peschon, J.J.; Torrance, D.S.; Stocking, K.L.; Glaccum, M.B.; Otten, C.; Willis, C.R.; Charrier, K.; Morrissey, P.J.; Ware, C.B.; Mohler, K.M. TNF Receptor-Deficient Mice Reveal Divergent Roles for p55 and p75 in Several Models of Inflammation. *J. Immunol.* **1998**, *160*, 943–952.

14. Davidson, W.F.; Calkins, C.; Hugins, A.; Giese, T.; Holmes, K.L. Cytokine secretion by C3H-lpr and -gld T cells. Hypersecretion of IFN-gamma and tumor necrosis factor-alpha by stimulated CD4+ T cells. *J. Immunol.* **1991**, *146*, 4138–4148.

15. Körner, H.; McMorran, B.; Schluter, D.; Fromm, P. The role of TNF in parasitic diseases: Still more questions than answers. *Int. J. Parasitol.* **2010**, *40*, 879–888.

16. Efimov, G.A.; Kruglov, A.A.; Tillib, S.V.; Kuprash, D.V.; Nedospasov, S.A. Tumor Necrosis Factor and the consequences of its ablation *in vivo*. *Mol. Immunol.* **2009**, *47*, 19–27.

17. Chen, X.; Oppenheim, J.J. TNF-alpha: An activator of CD4+FoxP3+TNFR2+ regulatory T cells. *Curr. Dir. Autoimmun.* **2010**, *11*, 119–134.

18. Andrews, B.S.; Eisenberg, R.A.; Theofilopoulos, A.N.; Izui, S.; Wilson, C.B.; McConahey, P.J.; Murphy, E.D.; Roths, J.B.; Dixon, F.J. Spontaneous murine lupus-like syndromes. Clinical and immunopathological manifestations in several strains. *J. Exp. Med.* **1978**, *148*, 1198–1215.

19. Dixon, F.J.; Andrews, B.S.; Eisenberg, R.A.; McConahey, P.J.; Theofilopoulos, A.N.; Wilson, C.B. Etiology and pathogenesis of a spontaneous lupus-like syndrome in mice. *Arthrits Rheum.* **1978**, *21*, S64–S67.

20. Teh, H.-S.; Seebaran, A.; Teh, S.-J. TNF Receptor 2-Deficient CD8 T Cells Are Resistant to Fas/Fas Ligand-Induced Cell Death. *J. Immunol.* **2000**, *165*, 4814–4821.

21. Cheng, G.; Baltimore, D. TANK, a co-inducer with TRAF2 of TNF- and CD 40L-mediated NF-kappaB activation. *Genes Dev.* **1996**, *10*, 963–973.

22. Van Antwerp, D.J.; Martin, S.J.; Kafri, T.; Green, D.R.; Verma, I.M. Suppression of TNF-alpha-induced apoptosis by NF-kappaB. *Science* **1996**, *274*, 787–789.

23. Körner, H.; Cook, M.; Riminton, D.S.; Lemckert, F.A.; Hoek, R.M.; Ledermann, B.; Köntgen, F.; Fazekas de St Groth, B.; Sedgwick, J.D. Distinct roles for lymphotoxin-alpha and tumor necrosis factor in organogenesis and spatial organization of lymphoid tissue. *Eur. J. Immunol.* **1997**, *27*, 2600–2609.

24. Pasparakis, M.; Alexopoulou, L.; Grell, M.; Pfizenmaier, K.; Bluethmann, H.; Kollias, G. Peyer's patch organogenesis is intact yet formation of B lymphocyte follicles is defective in peripheral lymphoid organs of mice deficient for tumor necrosis factor and its 55-kDa receptor. *Proc. Natl. Acad. Sci. USA* **1997**, *94*, 6319–6323.

25. Körner, H.; Winkler, T.H.; Sedgwick, J.D.; Röllinghoff, M.; Basten, A.; Cook, M.C. Recirculating and marginal zone B cell populations can be established and maintained independently of primary and secondary follicles. *Immunol. Cell Biol.* **2001**, *79*, 54–61.

26. Asano, T.; Tomooka, S.; Serushago, B.A.; Himeno, K.; Nomoto, K. A new T cell subset expressing B220 and CD4 in lpr mice: Defects in the response to mitogens and in the production of IL-2. *Clin. Exp. Immunol.* **1988**, *74*, 36–40.

27. Ansel, K.M.; McHeyzer-Williams, L.J.; Ngo, V.N.; McHeyzer-Williams, M.G.; Cyster, J.G. *In vivo*-activated CD4 T cells upregulate CXC chemokine receptor 5 and reprogram their response to lymphoid chemokines. *J. Exp. Med.* **1999**, 1123–1134.

28. Hoek, R.C.; Kortekaas, M.C.; Sedgwick, J.D. Allele-specific PCR analysis for detection of the *gld* Fas-ligand point mutation. *J. Immunol. Methods* **1997**, *210*, 109–112.

29. Ritter, U.; Wiede, F.; Mielenz, D.; Kiafard, Z.; Zwirner, J.; Körner, H. Analysis of the CCR7 expression on murine bone marrow-derived and spleen dendritic cells. *J. Leukoc. Biol.* **2004**, *76*, 472–476.

30. Hodgkin, P.D.; Lee, J.H.; Lyons, A.B. B cell differentiation and isotype switching is related to division cycle number. *J. Exp. Med.* **1996**, *184*, 277–281.